analytical chemistry

pubs.acs.org/ac Article

Electrochemical Biosensor with Enhanced Antifouling Capability Based on Amyloid-like Bovine Serum Albumin and a Conducting Polymer for Ultrasensitive Detection of Proteins in Human Serum

Yang Li, Rui Han, Min Chen, Xiqin Yang, Yinan Zhan, Lei Wang, and Xiliang Luo*

Cite This: *Anal. Chem.* 2021, 93, 14351−14357 Read Online

ACCESS | Metrics & More | Article Recommendations | Supporting Information

ABSTRACT: Biofouling has been a substantial burden on biomarker analysis in complex biological media, leading to poor sensitivity and selectivity or even malfunction of the sensing devices. In this work, an electrochemical biosensor with excellent antifouling ability and high stability was fabricated based on amyloid-like bovine serum albumin (AL-BSA) crosslinked with the conducting polymer polyaniline (PANI). Compared with the crosslinked conventional bovine serum albumin (BSA), the crosslinked AL-BSA exhibited enhanced antifouling capability, and it was able to form an effective antifouling film within a significantly short reaction time. With further immobilization of immunoglobulin M (IgM) antibodies onto the prepared AL-BSA surface via the formation of amide bonds, an electrochemical biosensor capable of assaying IgM in human serum samples with superior selectivity and sensitivity was constructed. The biosensor exhibited excellent antifouling performance even in 100% human serum, a low limit of detection down to 2.32 pg mL^{-1}, and acceptable accuracy for real sample analysis compared with the standard enzyme-linked immunosorbent assay for IgM detection. This strategy of using AL-BSA to construct antifouling sensing interfaces provided a reliable diagnostic method for the detection of a series of protein biomarkers in complex biological media.

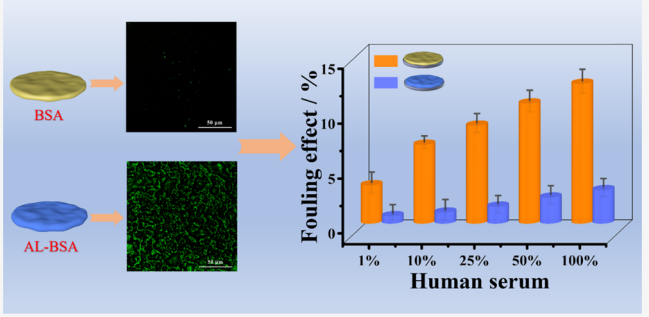

Biosensors performing in complex biological fluids are prone to be affected by various contaminants (such as proteins, cells, and polyoses) that adhered to the sensing interfaces, resulting in the degradation in sensitivity and specificity and even malfunction of biosensors.[1] Mounting evidence indicates that biofouling is an undesirable phenomenon for biosensors performed in complex biological media, which has been considered to result from the nonspecific adsorption of macromolecules or biological substances.[2,3] Consequently, preventing various contaminations is of vital significance for the application of biosensors in real samples to detect and monitor different biomarkers.

To alleviate the issue of biofouling, various kinds of materials have been selected and integrated onto the sensing interfaces of biosensors to effectively reduce nonspecific adsorption.[4,5] To date, different materials including zwitterionic materials,[6,7] poly(ethylene glycol) (PEG),[8,9] peptides and peptoids,[10−12] and hyaluronic acid (HA)[13] have been explored to deal with biofouling issues. Although enormous progress has been made in the development of antifouling biosensors based on these materials, they still have some drawbacks. For instance, PEGs are easily degradable by certain enzymes and susceptible to oxidative damage in biological environments,[14] and the peptide synthesis generally requires a complicated process,[15] which greatly limited their practical application. Therefore, the search for stable and cost-effective antifouling materials is of fundamental importance to construct effective antifouling biosensors.

Bovine serum albumin (BSA), as the widely available protein component of plasma, exhibits the function of providing pH buffering and maintaining the osmotic blood pressure and has been widely used as a carrier to deliver drugs and small active molecules, owing to its abundance, cost-effectiveness, and ease of passivation.[16,17] In many cases, BSA, as an inexpensive choice, was used as a passivator to block active sites of the sensing interfaces and to resist nonspecific adsorption in biological environments.[18−20] Besides normal physical adsorption of BSA, our group has also constructed a biosensor based on BSA-crosslinked conducting polymer nanowires recently, which exhibited high sensitivity and excellent antifouling capability.[21]

Amyloid proteins tend to deposit in a variety of cells or tissues as aggregates with unique fibrillary microstructures, and

Received: September 24, 2021
Accepted: October 1, 2021
Published: October 14, 2021

the accumulation of the amyloid protein has been found to be associated with Alzheimer's disease.[22] Recently, Yang's group has reported that the reduction of intramolecular disulfide bonds of BSA with tris(2-carboxyethyl)phosphine (TCEP) resulted in the formation of amyloid-like protein aggregates, and the phase-transited BSA exhibited superior antifouling capability even in harsh conditions.[23] In the light of this interesting work, we herein constructed a novel antifouling electrochemical biosensor for the detection of proteins in biological media based on amyloid-like BSA (AL-BSA). Considering the poor conductivity of AL-BSA, we electrodeposited the conducting polymer polyaniline (PANI) on the electrode surface to enhance the current signal of the biosensor using differential pulse voltammetry (DPV) as a general electrochemical sensing approach. AL-BSA was crosslinked with PANI to form a substrate with both high conductivity and superior antifouling capability, which is preferred for the construction of antifouling electrochemical biosensors. Immunoglobulin M (IgM), commonly regarded as an important biomarker of disease diagnosis and one of the indicators of COVID-19,[24] was selected as a typical target, and the IgM antibody was attached to the AL-BSA-/PANI-modified electrode for the fabrication of an antifouling electrochemical IgM biosensor. The fabricated biosensor was capable of assaying IgM in complicated biological media (such as human serum and blood) without biofouling and with reliable accuracy.

EXPERIMENTAL SECTION

Reagents. BSA was purchased from Adamas-Beta Reagent (Shanghai, China). Tris(2-carboxyethyl)phosphine hydrochloride (TCEP) and fluorescein diacetate (FDA) were provided by Sangon Biotech Co., Ltd. (Shanghai, China). Thioflavin-T (ThT) was provided by Sigma-Aldrich. Aniline was provided by Aladdin Reagent Co., Ltd. (Shanghai, China). Glutaraldehyde (GA), 1-(3-dimethylaminopropyl)-3-ethylcarbodiimide hydrochloride (EDC), and *N*-hydroxysuccinimde (NHS) were obtained from Macklin Biochemical Co., Ltd. Anti-IgM antibody (Ab), human immunoglobulin M (IgM), human immunoglobulin G (IgG), 2019-nCoV receptor-binding domain (RBD), carbohydrate antigen 15-3 (CA15-3), carbohydrate antigen 125 (CA125), α-fetoprotein (AFP), carcinoembryonic antigen (CEA), and human epidermal growth factor receptor 2 (HER2) were obtained from Solarbio Co., Ltd. (Beijing, China). Cell culture was performed with the Roswell Park Memorial Institute 1640 medium (RPMI-1640 medium) from Sigma Co., Ltd. (Aldrich, St. Louis, MO). Real human serum samples and human blood were provided by the Eighth People's Hospital of Qingdao (Qingdao, China). IgM concentrations from serum samples were measured by ELISA using commercial kits (Jiangsu Meimian Industrial Co., Ltd., Jiangsu, China). All other reagents were of analytical grade, and pure water (resistivity > 18 MΩ cm) was obtained from a Mill-Q purification system (Millipore, Bedford, MA).

Apparatus. Electrochemical measurements were performed with a CHI 660E electrochemical workstation (Shanghai, China) using a three-electrode system, with a glassy carbon electrode (GCE, diameter of 3.0 μm) as the working electrode, a platinum wire as the auxiliary electrode, and a saturated calomel electrode (SCE) as the reference electrode. Cell adsorption test and ThT staining assay were performed with a confocal microscope (Leica, Germany) to record their fluorescence images. Fluorescence spectra were recorded using a FL-4600 fluorescence spectrometer (Hitachi, Japan). Scanning electron microscopy (SEM) was carried out using a Hitachi Regulus 8100 SEM instrument (Hitachi Co., Ltd., Japan). The amyloid assembly of BSA was characterized with a JASCO J-810 spectropolarimeter (Jasco Inc., Japan) by recording the circular dichroism (CD) spectra. Element concentrations were monitored by X-ray photoelectron spectroscopy (XPS) using an ESCALAB 250Xi spectrometer (Thermo-VG Fisher Scientific), with a monochromatic Al Kα X-ray source ($h\nu$ = 15 kV), and the C 1s peak of 284.6 eV was used as a reference for all spectra. ELISA kit was used to analyze the concentration of IgM from real human serum samples, and the absorbance was recorded using an EPOCH2 microplate reader (BioTek Instruments, Winooski, VT).

Preparation and Characterization of AL-BSA. The amyloid-like BSA was prepared by mixing the BSA solution (2.0 mg mL^{-1}), TCEP solution (50 mM, pH 5.5, adjusted by NaOH), and phosphate-buffered saline (PBS, 10.0 mM, pH 7.4) with the volume ratio of 1:1:1 at room temperature. The BSA underwent amyloid aggregation and became oligomer nanoparticles and protofibrils.[25]

The charges of the native BSA and AL-BSA were characterized by measuring their ζ-potential. CD spectra were measured to demonstrate the successful phase transition of BSA in the wavelength range of 200−260 nm with a 0.2 nm bandwidth. BSA was diluted to 0.2 mg mL^{-1} and TCEP to 5.0 mM for the CD spectrum measurement.

The amyloid structure of AL-BSA was investigated by the cationic fluorescent dye ThT. AL-BSA was attached to the electrode surface, and the modified electrode was soaked in ThT aqueous solution (10.0 mM) in the dark environment for 15 min under quiescent conditions. The fluorescence signals of the native BSA and AL-BSA-modified electrodes after ThT staining were then measured by a fluorescence spectrophotometer, and the fluorescence images were monitored by the Leica confocal microscope, with the excitation and emission wavelengths at 440 and 484 nm, respectively.

Preparation of the PANI-Modified Electrode. After polishing with 1.0, 0.3, and 0.05 μm Al_2O_3 slurry, the GCE was ultrasonically washed with water, ethanol, and water, each for 2 min, successively. Subsequently, the GCE was immersed in 1.0 M $HClO_4$ aqueous solution containing 0.1 M aniline to electrochemically polymerize PANI through a galvanostatic technique with a current density of 0.01 mA cm^{-1} at room temperature for 50 min.

Preparation of Different BSA-/PANI-Modified Electrodes. Three electrodes modified with AL-BSA(physical adsorption)/PANI, BSA(GA crosslink)/PANI, and AL-BSA-(GA crosslink)/PANI were fabricated, and the effect of the reaction time of BSA on their antifouling performances was investigated. The AL-BSA(physical adsorption)/PANI-modified electrode was prepared via immersing the PANI-modified electrode in the AL-BSA solution (2.0 mg mL^{-1} BSA, 50 mM TCEP, and 10.0 mM PBS at a volume ratio of 1:1:1). The BSA(GA crosslink)/PANI-modified electrode was constructed by soaking the PANI-modified electrode in the BSA solution (2.0 mg mL^{-1} BSA, 10.0 mM PBS, and 5% GA at a volume ratio of 1:1:1). The AL-BSA(GA crosslink)/PANI-modified electrode was fabricated via immersing the PANI-modified electrode in the AL-BSA/GA solution (2.0 mg mL^{-1} BSA, 50 mM TCEP, and 5% GA at a volume ratio of 1:1:1). All of these modified electrodes were immersed in 100% human serum for half an hour at room temperature, and the antifouling

https://doi.org/10.1021/acs.analchem.1c04153
Anal. Chem. 2021, 93, 14351−14357

capabilities of these electrodes were evaluated by DPV. In addition, the long-term antifouling abilities of these electrodes soaked in 100% serum were also investigated.

Preparation of the Antifouling Biosensor. The fabrication process of the antifouling biosensor is illustrated in Scheme 1. The PANI-modified electrode was placed in the AL-BSA/GA solution at room temperature for 1 h, followed by washing with water. The carboxyl group of AL-BSA was activated by the EDC/NHS solution (containing 0.4 M EDC and 0.1 M NHS) for 0.5 h and then 15 μL of 2.0 μg mL^{-1} Ab was dropped onto the electrode surface for 2 h at room temperature. Ultimately, the antifouling biosensor was prepared by the formation of amide bonds between the carboxyl and amino groups (from Ab).

Scheme 1. Schematic Description of the Construction of the Antifouling IgM Biosensor Based on AL-BSA

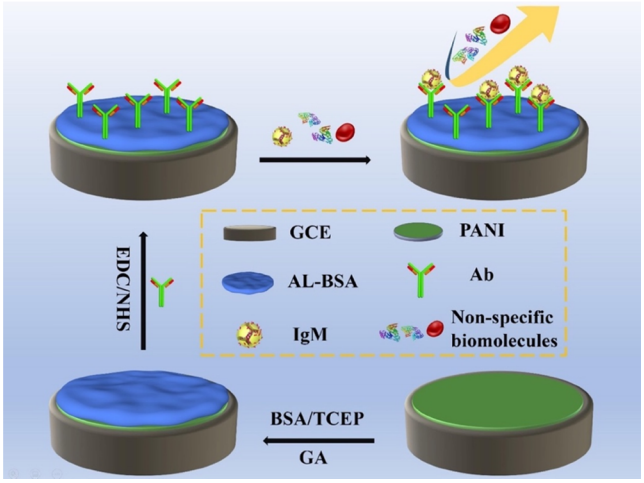

Characterization of the Antifouling Ability. The AL-BSA(physical adsorption)/PANI and BSA(GA crosslink)/PANI-modified electrodes (with the BSA adsorption/reaction time of 1 h) were used as controls, and other related experimental conditions were same as the AL-BSA(GA crosslink)/PANI-modified electrode. The antifouling capability of the PANI, AL-BSA(physical adsorption)/PANI, BSA(GA crosslink)/PANI, AL-BSA(GA crosslink)/PANI-modified electrodes, and the IgM biosensor was evaluated by measuring the changed DPV signals after soaking in different dilution ratio (v/v) solutions of human serum and blood (diluted with 10.0 mM PBS, pH 7.4) for 30 min, and the IgM biosensor was saturated with IgM (1.0 mg mL^{-1}) before the measurement.

In addition, the antifouling performance was further evaluated by a cell adhesion test. The newly reconstituted Michigan Cancer Foundation-7 (MCF-7) cells, a common kind of adherent cells, were resuspended in RPMI-1640 medium and then collected by centrifugation. Subsequently, the PANI, AL-BSA(GA crosslink)/PANI-modified surfaces, and the IgM biosensor were incubated with MCF-7 cells for 24 h (37 °C, 5% CO_2) and followed by washing with Dulbecco's phosphate-buffered saline (DPBS) to remove unattached cells. The samples were characterized by fluorescence microscopy

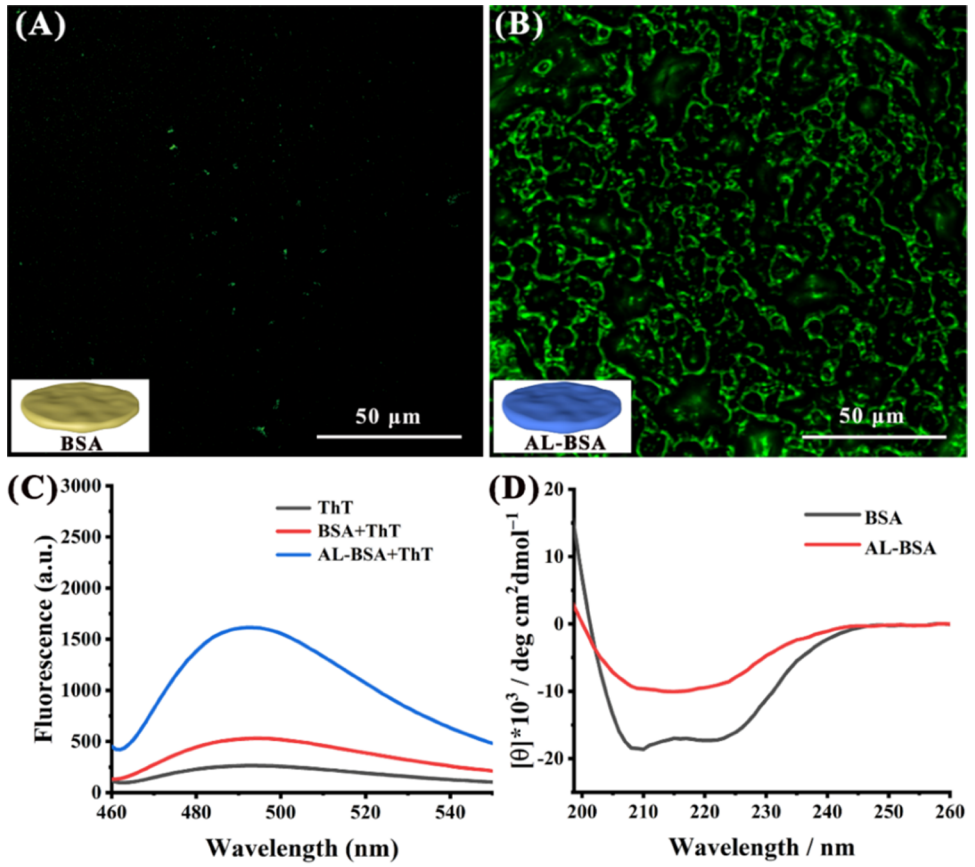

Figure 1. Fluorescence images of (A) the native BSA and (B) AL-BSA coated on the electrodes after ThT staining. (C) Fluorescence spectra of the ThT, BSA, and AL-BSA aqueous solutions stained with ThT. (D) CD spectra of 0.2 mg mL^{-1} native BSA and AL-BSA solutions.

https://doi.org/10.1021/acs.analchem.1c04153
Anal. Chem. 2021, 93, 14351−14357

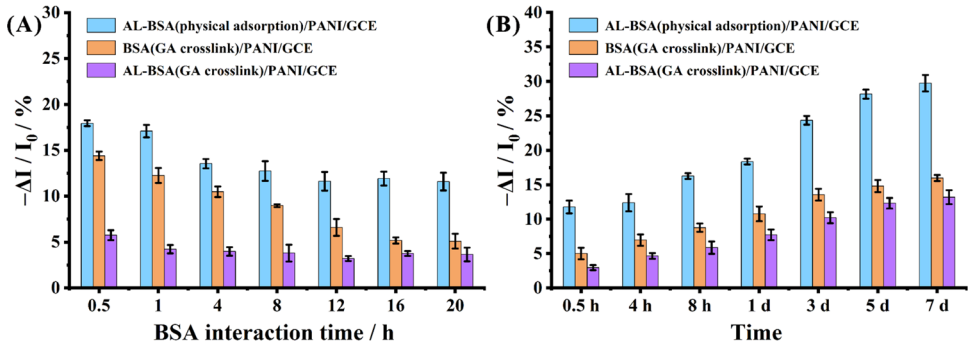

Figure 2. (A) Antifouling performances of the AL-BSA(physical adsorption)/PANI/GCE, BSA(GA crosslink)/PANI/GCE, and AL-BSA(GA crosslink)/PANI/GCE in undiluted human serum under different BSA reaction/adsorption time. (B) Long-term antifouling abilities of three modified electrodes soaked in undiluted human serum. Error bars represent the standard deviations of three repeated determinations.

with an excitation wavelength at 488 nm, stained with fluorescein diacetate (FDA).

Detection of IgM. The prepared antifouling biosensors were immersed in different concentrations of IgM solutions (diluted by 10.0 mM PBS, pH 7.4) for 60 min at 37 °C, and the signal changes were measured by DPV. The DPV detection was performed with the scanning potential from −0.6 to 0.6 V at the amplitude of 50 mV, with the pulse period of 0.2 s and the potential increment of 4.0 mV.

For real serum analysis, the serum samples from the fresh blood of seven people were collected by centrifugation for 5 min at 10 000 rpm. Subsequently, the contents of IgM in the serum samples were quantitatively analyzed with the prepared IgM biosensor and the commercial ELISA kits, respectively. The results detected with the biosensors were compared with those measured with the ELISA kits, so as to verify the accuracy and reliability of the developed IgM biosensor.

RESULTS AND DISCUSSION

Characterization of AL-BSA. The amyloid assembly process and the secondary structure of AL-BSA were characterized by fluorescence and CD spectroscopy. The formation of AL-BSA was checked by the ThT assay, which was an established method to indicate the amyloid assembly.[26] The amyloid assembly process of BSA induced by TCEP was verified by the fluorescence images of AL-BSA and native BSA recorded at the emission wavelength of 484 nm (Figures 1A,B and S1). Clearly, AL-BSA exhibited significantly enhanced fluorescence after ThT staining, associated with the binding of ThT on β-sheet structures. In addition, the fluorescence intensity of BSA and AL-BSA was measured after ThT staining, as shown in Figure 1C. Compared with the native BSA, the fluorescence intensity of AL-BSA was remarkably enhanced around the wavelength of 490 nm, indicating that the β-sheet structure of AL-BSA increased significantly. The amyloid assembly process suggested that the changes observed in the fluorescence intensity were correlated with the secondary structure change of BSA, which was further demonstrated by the CD spectrum (Figure 1D). It was clearly observed that BSA showed two peaks at about 208 and 222 nm, associated with the α-helix structure of proteins, while AL-BSA showed a single peak at about 216 nm related to the β-sheet structure of proteins. These results revealed the changes in the secondary structure of BSA and the successful formation of AL-BSA.[23]

Antifouling Performances of Different BSA/PANI-Modified Electrodes. The AL-BSA(physical adsorption)/PANI, BSA(GA crosslink)/PANI, and AL-BSA(GA crosslink)/PANI-modified electrodes were prepared, and the effect of the reaction/adsorption time of BSA on their antifouling performances in undiluted human serum was explored (Figure 2A). The current signal of the AL-BSA(physical adsorption)/PANI and BSA(GA crosslink)/PANI-modified electrodes significantly decreased along with the extension of time, and the stable antifouling performances were achieved after about 16 h, with the signal change rates of 11.6 and 5.3%, respectively. By contrast, the signal of the AL-BSA(GA crosslink)/PANI-modified electrode was more stable, and it was less than 5.0% after a reaction time of just 1 h, indicating that AL-BSA(GA crosslink)/PANI-modified electrode was able to achieve excellent antifouling property in a very short time compared with other modified electrodes. That is, the GA crosslinked AL-BSA with superior antifouling ability in human serum and excellent stability can be prepared within 1 h, which is suitable for application in complex biological environments such as human serum and sweat.

Furthermore, the long-term antifouling properties of these three modified electrodes (under optimized BSA reaction/adsorption time) in undiluted serum were investigated and are shown in Figure 2B. Clearly, the AL-BSA(GA crosslink)/PANI-modified electrode exhibited the best antifouling performance, and even after soaking in 100% human serum for 4 h (most of the bioassays can be finished within such a time period), the signal change rate was less than 5.0%, indicating a promising potential of this antifouling biosensor for practical applications.

Construction of the Antifouling Biosensor. The concentration of BSA and the reaction time of BSA with TCEP to form AL-BSA were optimized to obtain better antifouling property, and finally, the conditions of 2.0 mg mL^{-1} and 1 h were selected (Figure S2). In addition, SEM was used to characterize the morphologies of different modified electrodes. The surface of PANI/GCE shows the morphology of nanoparticles with diameters of 50−100 nm, which can provide a surface with excellent conductivity for the subsequent modification of AL-BSA (Figure S3A). After crosslinking with AL-BSA, a layer of a uniform AL-BSA film on the PANI surface was observed (Figure S3B). Similarly, the pure AL-BSA-modified electrode surface also showed a uniform film with homogeneous morphology (Figure S3C).

To verify the successful attachment of AL-BSA onto the electrode surface, the elemental compositions of different modified electrode surfaces were characterized by XPS (Figure S4). Different from the C 1s, O 1s, and N 1s photoelectron signals observed on the PANI-modified electrode, the AL-

https://doi.org/10.1021/acs.analchem.1c04153
Anal. Chem. 2021, 93, 14351−14357

BSA(GA crosslink)/PANI-modified electrode exhibited an additional photoelectron signal of S 2p (163 eV), owing to the presence of AL-BSA. In addition, the photoelectron peak of N 1s of the AL-BSA(GA crosslink)/PANI-modified electrode was also increased significantly. These results demonstrated that AL-BSA was successfully attached to PANI/GCE.

The fabrication process of the IgM biosensor was characterized by DPV (Figure 3). Due to the outstanding

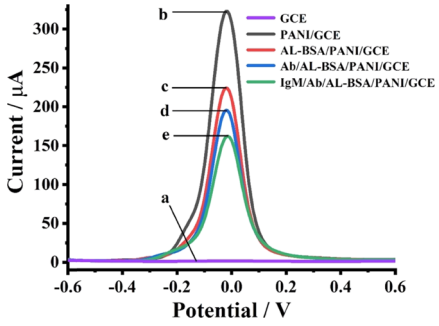

Figure 3. Electrochemical responses of different modified electrodes in PBS (0.2 mM, pH 7.4). AL-BSA is crosslinked to the PANI-modified electrode via GA during the fabrication of the biosensor.

conductivity of PANI, the current signal was markedly enhanced after PANI is electrodeposited on the bare electrode (Figure 3, curves a, b). Subsequently, due to the clogging effect and poor conductivity of AL-BSA, the current signal of the AL-BSA/PANI-modified electrode was significantly reduced (Figure 3, curve c). Furthermore, the immobilization of Ab blocked the charge transfer, leading to a decrease in the current signal (Figure 3, curve d). Finally, owing to the steric hindrance effect, the current signal was further reduced after the IgM was captured (Figure 3, curve e). Therefore, these results proved the successful fabrication of the biosensor, and the current change after IgM binding represented the biosensing signal.

Investigation of the Antifouling Performance. A series of human serum and blood samples were applied to investigate the antifouling properties of different modified electrodes, and the relevant DPV signal changes are elucidated in Figure S5. As displayed in Figure 4, the current signal change rates of the PANI, AL-BSA(physical adsorption)/PANI, and BSA(GA crosslink)/PANI-modified electrodes in 100% human serum were decreased by 23.9, 15.4, and 12.8%, respectively, owing to the biofouling of serum. In contrast, the signal of the AL-BSA(GA crosslink)/PANI-modified electrode and the IgM biosensor was decreased slightly by 2.9 and 3.3%, respectively. Similarly, the AL-BSA(GA crosslink)/PANI-modified electrode and the IgM biosensor also maintained excellent antifouling abilities (signal change rates were less than 5%) in 100% human blood. The excellent antifouling properties of AL-BSA(GA crosslink)/PANI/GCE and the IgM biosensor were ascribed to the presence of AL-BSA, which was tightly attached to the electrode surfaces through the GA crosslinking. The outstanding antifouling ability of AL-BSA was originated from the amino acid residues with positive and negative charges that were almost evenly distributed over the surface of AL-BSA, and this fact was also verified by the ζ-potential.[27] As shown in Figure S6, there was a strong negative charge of the native BSA, while AL-BSA exhibited a very weak negative charge, which was preferred for antifouling materials so as to prevent nonspecific adsorption caused by the charge attraction.

Additionally, to further evaluate the antifouling performance, a cell adhesion test was carried out using MCF-7 cells (Figure S7). Compared with the PANI-modified electrode that showed a large amount of attached cells, the AL-BSA(GA crosslink)/PANI-modified electrode and the IgM biosensor were able to resist cell adhesion, and there were few cells adsorbed on their modified surfaces.

Electrochemical Detection of the Target IgM. The incubation time of the biosensor to capture the antibody was investigated to obtain the best sensing performance, and finally, 60 min was selected as the optimal incubation time (Figure S8). Under optimized sensing conditions, the biosensor response to IgM is shown in Figure 5A,B, and the relevant DPV responses are shown in Figure S9. The linear fitting equation of the electrochemical biosensor was obtained as $-\Delta I$ (μA) = 4.84 lg(C) + 43.75 (R^2 = 0.9975), within the linear range of 10.0 pg mL^{-1} to 10.0 μg mL^{-1}. The limit of detection (LOD) of the biosensor was calculated to be 2.32 pg mL^{-1}, which was much lower than the LODs of the previously reported IgM biosensor (Table S1).[28−31] The low LOD may be due to the superiority of the AL-BSA-modified electrode with outstanding stability and excellent antifouling capability, which provides a low noise signal for high specificity of IgM.

In addition, the antifouling sensing ability of the biosensor was also examined in 100% fetal bovine serum (FBS), as

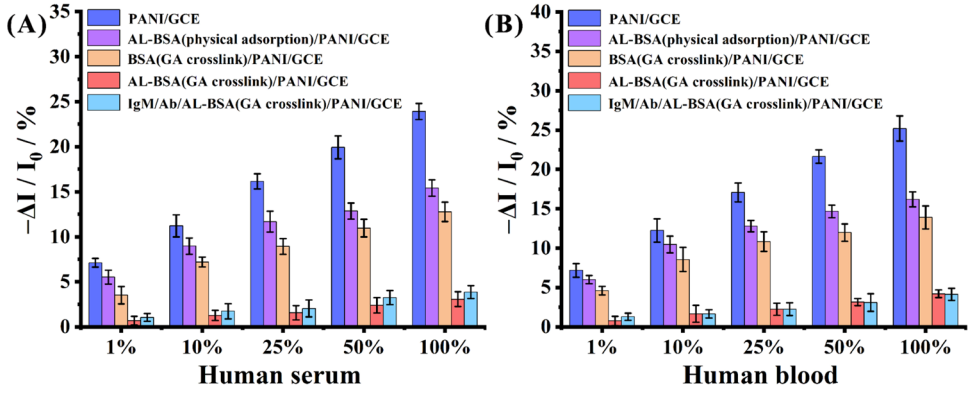

Figure 4. Comparison of antifouling properties of PANI/GCE, AL-BSA(physical adsorption)/PANI/GCE, BSA(GA crosslink)/PANI/GCE, AL-BSA(GA crosslink)/PANI/GCE, and IgM/Ab/AL-BSA(GA crosslink)/PANI/GCE in different concentrations of (A) human serum and (B) human blood samples.

https://doi.org/10.1021/acs.analchem.1c04153
Anal. Chem. 2021, 93, 14351−14357

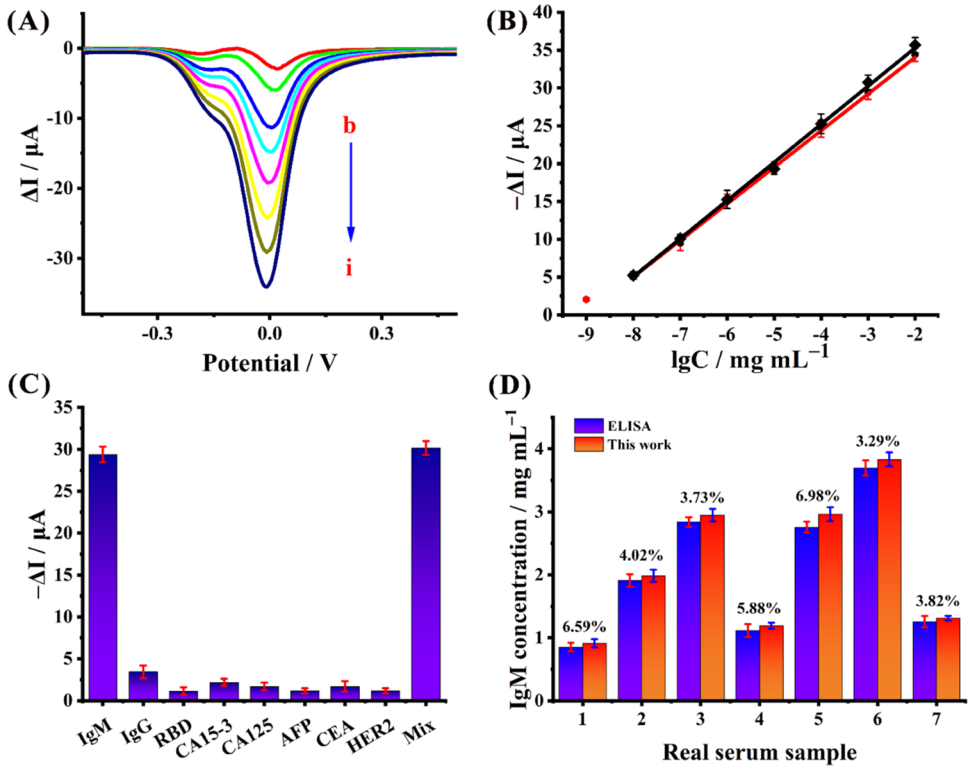

Figure 5. (A) DPV curves after background subtraction. Curves (b−i) corresponding to IgM at concentrations from 10.0 pg mL^{-1} to 10.0 μg mL^{-1}. (B) Linear calibration curves of the biosensor for IgM detection in 10.0 mM PBS (red) and 100% FBS (black). (C) Responses of the IgM biosensor to 1.0 μg mL^{-1} IgM, 1.0 mg mL^{-1} of IgG, RBD, CA15-3, CA125, AFP, CEA, HER2, and a mixture (Mix) of the above proteins. (D) Results of real serum samples are measured by the ELISA assay and the biosensor.

displayed in Figure 5B. The linear fitting equation was obtained as $-\Delta I$ (μA) = 5.04 lg(C) + 45.37, which is close to that in pure PBS. The results exhibited that the detection performance of biosensors was almost unaffected in complex biological media, indicating the promising potential for clinical applications.

Selectivity and Reproducibility of the Antifouling Biosensor. The selectivity of the fabricated IgM biosensor was investigated in the presence of various interfering proteins. A series of proteins were selected, including IgG, RBD, CA15-3, CA125, AFP, CEA, and HER2 (Figure 5C). The results reflected that the biosensor exhibited a superior response to the target IgM, and the specific target was detected accurately in the mixed samples. Meanwhile, the response to the interfering proteins was almost negligible, and even in the absence of much higher concentrations of various interferences, indicating excellent selectivity of the IgM biosensor.

Stability analysis for the prepared biosensor was carried out in PBS (0.2 M, pH 7.4), and the DPV signal was measured every 30 min for nine times. The signal responses of the IgM biosensor were almost unchanged, which indicated excellent stability of the biosensor based on AL-BSA (Figure S10A). In addition, the reproducibility of the antifouling biosensor was also investigated (Figure S10B). For the detection of IgM, the relative standard deviation of the responses of nine independently prepared electrodes was 0.33%, demonstrating excellent reproducibility.

Clinical Serum Sample Analysis. To evaluate the practical application ability of the antifouling biosensor, seven serum samples provided by the hospital were tested with the biosensor, and the results were then compared with the IgM concentrations determined by the ELISA method (Figure 5D). There were small differences between the IgM concentrations measured with the biosensor and ELISA assay (within 7%), which indicated that the IgM contents obtained by the biosensor were highly consistent with those obtained by the ELISA method. These results revealed the promising practical application prospect of the biosensor for clinical detection of various biomarkers based on the excellent antifouling performance of AL-BSA.

CONCLUSIONS

In conclusion, an innovative antifouling electrochemical biosensor based on AL-BSA crosslinked with PANI was developed. Compared with the native BSA-modified electrode, the AL-BSA(GA crosslink)/PANI-modified electrode displayed outstanding antifouling performance, superior conductivity, and high selectivity and sensitivity. Owing to its excellent antifouling property in complex biological samples, the biosensor was capable of detecting target IgM in real human serum with satisfactory accuracy, which was verified by the standard ELISA assay. This strategy of constructing a biosensor with superior antifouling capability and excellent sensitivity provided a promising approach for the development of other biosensors for biomarker detection in complex biological media.

ASSOCIATED CONTENT

Supporting Information

The Supporting Information is available free of charge at https://pubs.acs.org/doi/10.1021/acs.analchem.1c04153.

https://doi.org/10.1021/acs.analchem.1c04153
Anal. Chem. 2021, 93, 14351−14357

Fluorescence images; optimization of the experiment conditions; SEM images; XPS characterization; ζ-potential; optimization of incubation time of target, stability, and reproducibility of the biosensor; and comparison of different IgM assaying methods (PDF)

AUTHOR INFORMATION

Corresponding Author

Xiliang Luo − *Key Laboratory of Optic-Electric Sensing and Analytical Chemistry for Life Science, MOE, Shandong Key Laboratory of Biochemical Analysis, College of Chemistry and Molecular Engineering, Qingdao University of Science and Technology, Qingdao 266042, China;* orcid.org/0000-0001-6075-7089; Phone: +86 53284022860; Email: xiliangluo@qust.edu.cn; Fax: +8653284022681

Authors

Yang Li − *Key Laboratory of Optic-Electric Sensing and Analytical Chemistry for Life Science, MOE, Shandong Key Laboratory of Biochemical Analysis, College of Chemistry and Molecular Engineering, Qingdao University of Science and Technology, Qingdao 266042, China*

Rui Han − *Key Laboratory of Optic-Electric Sensing and Analytical Chemistry for Life Science, MOE, Shandong Key Laboratory of Biochemical Analysis, College of Chemistry and Molecular Engineering, Qingdao University of Science and Technology, Qingdao 266042, China*

Min Chen − *Key Laboratory of Optic-Electric Sensing and Analytical Chemistry for Life Science, MOE, Shandong Key Laboratory of Biochemical Analysis, College of Chemistry and Molecular Engineering, Qingdao University of Science and Technology, Qingdao 266042, China*

Xiqin Yang − *Key Laboratory of Optic-Electric Sensing and Analytical Chemistry for Life Science, MOE, Shandong Key Laboratory of Biochemical Analysis, College of Chemistry and Molecular Engineering, Qingdao University of Science and Technology, Qingdao 266042, China*

Yinan Zhan − *Key Laboratory of Optic-Electric Sensing and Analytical Chemistry for Life Science, MOE, Shandong Key Laboratory of Biochemical Analysis, College of Chemistry and Molecular Engineering, Qingdao University of Science and Technology, Qingdao 266042, China*

Lei Wang − *Key Laboratory of Optic-Electric Sensing and Analytical Chemistry for Life Science, MOE, Shandong Key Laboratory of Biochemical Analysis, College of Chemistry and Molecular Engineering, Qingdao University of Science and Technology, Qingdao 266042, China*

Complete contact information is available at: https://pubs.acs.org/10.1021/acs.analchem.1c04153

Notes

The authors declare no competing financial interest.

ACKNOWLEDGMENTS

This work was financially supported by the National Natural Science Foundation of China (21974075, 21675093), the Taishan Scholar Program of Shandong Province of China (ts20110829), and the Science and Technology Benefiting the People Project of Qingdao (20-3-4-53-nsh).

REFERENCES

(1) Lin, P.-H.; Li, B.-R. *Analyst* **2020**, *145*, 1110−1120.
(2) Jiang, C.; Wang, G.; Hein, R.; Liu, N.; Luo, X.; Davis, J. J. *Chem. Rev.* **2020**, *120*, 3852−3889.
(3) Sabaté del Río, J.; Henry, O. Y. F.; Jolly, P.; Ingber, D. E. *Nat. Nanotechnol.* **2019**, *14*, 1143−1149.
(4) Campuzano, S.; Pedrero, M.; Yanez-Sedeno, P.; Pingarron, J. M. *Int. J. Mol. Sci.* **2019**, *20*, No. 423.
(5) Vanova, V.; Mitrevska, K.; Milosavljevic, V.; Hynek, D.; Richtera, L.; Adam, V. *Biosens. Bioelectron.* **2021**, *180*, No. 113087.
(6) Izquierdo-Barba, I.; Colilla, M.; Vallet-Regí, M. *Acta Biomater.* **2016**, *40*, 201−211.
(7) He, M.; Gao, K.; Zhou, L.; Jiao, Z.; Wu, M.; Cao, J.; You, X.; Cai, Z.; Su, Y.; Jiang, Z. *Acta Biomater.* **2016**, *40*, 142−152.
(8) Lowe, S.; O'Brien-Simpson, N. M.; Connal, L. A. *Polym. Chem.* **2015**, *6*, 198−212.
(9) Hui, N.; Sun, X.; Niu, S.; Luo, X. *ACS Appl. Mater. Interfaces* **2017**, *9*, 2914−2923.
(10) Ham, H. O.; Park, S. H.; Kurutz, J. W.; Szleifer, I. G.; Messersmith, P. B. *J. Am. Chem. Soc.* **2013**, *135*, 13015−13022.
(11) Han, R.; Wang, G.; Xu, Z.; Zhang, L.; Li, Q.; Han, Y.; Luo, X. *Biosens. Bioelectron.* **2020**, *164*, No. 112317.
(12) Chen, M.; Song, Z.; Han, R.; Li, Y.; Luo, X. *Biosens. Bioelectron.* **2021**, *178*, No. 113016.
(13) Huang, R.; Liu, X.; Ye, H.; Su, R.; Qi, W.; Wang, L.; He, Z. *Langmuir* **2015**, *31*, 12061−12070.
(14) Du, Y.; Gao, J.; Chen, T.; Zhang, C.; Ji, J.; Xu, Z.-K. *Langmuir* **2017**, *33*, 7298−7304.
(15) Schwieter, K. E.; Johnston, J. N. *J. Am. Chem. Soc.* **2016**, *138*, 14160−14169.
(16) Bhattacharya, M.; Jain, N.; Mukhopadhyay, S. *J. Phys. Chem. B* **2011**, *115*, 4195−4205.
(17) Ma, G. J.; Ferhan, A. R.; Jackman, J. A.; Cho, N.-J. *Langmuir* **2020**, *36*, 10606−10614.
(18) Sweryda-Krawiec, B.; Devaraj, H.; Jacob, G.; Hickman, J. J. *Langmuir* **2004**, *20*, 2054−2056.
(19) Park, J. H.; Jackman, J. A.; Ferhan, A. R.; Ma, G. J.; Yoon, B. K.; Cho, N.-J. *ACS Appl. Mater. Interfaces* **2018**, *10*, 32047−32057.
(20) Wang, G.; Han, R.; Li, Q.; Han, Y.; Luo, X. *Anal. Chem.* **2020**, *92*, 7186−7193.
(21) Li, Y.; Han, R.; Chen, M.; Zhang, L.; Wang, G.; Luo, X. *Anal. Chem.* **2021**, *93*, 4326−4333.
(22) Ma, M.; Liu, Z.; Gao, N.; Pi, Z.; Du, X.; Ren, J.; Qu, X. *J. Am. Chem. Soc.* **2020**, *142*, 21702−21711.
(23) Hu, X.; Tian, J.; Li, C.; Su, H.; Qin, R.; Wang, Y.; Cao, X.; Yang, P. *Adv. Mater.* **2020**, *32*, No. 2000128.
(24) Hou, H.; Wang, T.; Zhang, B.; Luo, Y.; Mao, L.; Wang, F.; Wu, S.; Sun, Z. *Clin. Transl. Immunol.* **2020**, *9*, No. e1136.
(25) Li, C.; Xu, L.; Zuo, Y. Y.; Yang, P. *Biomater. Sci.* **2018**, *6*, 836−841.
(26) Chimon, S.; Ishii, Y. *J. Am. Chem. Soc.* **2005**, *127*, 13472−13473.
(27) Chen, S.; Cao, Z.; Jiang, S. *Biomaterials* **2009**, *30*, 5892−5896.
(28) Jiang, Z.; Wei, L.; Zou, M.; Liang, A.; Meng, M. *J. Biomol. Screening* **2008**, *13*, 302−308.
(29) Regiart, M.; Pereira, S. V.; Bertolino, F. A.; Garcia, C. D.; Raba, J.; Aranda, P. R. *Microchim. Acta* **2016**, *183*, 1203−1210.
(30) Ortega, G. A.; Zuaznabar-Gardona, J. C.; Reguera, E. *Biosens. Bioelectron.* **2018**, *116*, 30−36.
(31) Abad-Villar, E. M.; Tanyanyiwa, J.; Fernández-Abedul, M. T.; Costa-García, A.; Hauser, P. C. *Anal. Chem.* **2004**, *76*, 1282−1288.